

Charge ordering and hopping in a triangular array of quantum dots

L. S. Levitov¹, Boris Kozinsky

Center for Materials Science & Engineering, Physics Department, Massachusetts Institute of Technology

¹ *Also, Department of Condensed Matter Physics, The Weizmann Institute of Science, Rehovot 76100, Israel*

(October 7, 2018)

We demonstrate a mapping between the problem of charge ordering in a triangular array of quantum dots and a frustrated Ising spin model. Charge correlation in the low temperature state is characterized by an intrinsic height field order parameter. Different ground states are possible in the system, with a rich phase diagram. We show that electronic hopping transport is sensitive to the properties of the ground state, and describe the singularities of hopping conductivity at the freezing into an ordered state.

Ordering and phase transitions in artificial structures such as Josephson junction arrays [1] and arrays of quantum dots [2] have a number of interesting properties. One attractive feature of these systems is the control on the Hamiltonian by the system design. Also, the experimental techniques available for probing magnetic flux or charge ordering, such as electrical transport measurements and scanning probes, are more diverse and flexible than those conventionally used to study magnetic or structural ordering in solids. There has been a lot of theoretical [3] and experimental [1] studies of phase transitions and collective phenomena in Josephson arrays, and also some work on the quantum dot arrays [4,5].

There is an apparent similarity between the Josephson and the quantum dot arrays problems, because the former problem can be mapped using a duality transformation on the problem of charges on a dual lattice. These charges interact via the $D = 2$ Coulomb logarithmic potential, and can exhibit a Kosterlitz-Thouless transition, as well as other interesting first and second order transitions [3]. In the quantum dots arrays, charges are coupled via the $D = 3$ Coulomb $1/r$ potential, which can be also partially screened by ground electrodes or gates. In terms of the interaction range, the quantum dot array system is intermediate between the Josephson array problem and the lattice gas problems with short range interactions, such as the Ising model and its varieties. From that point of view, an outstanding question is what are the new physics aspects of this problem.

A very interesting system fabricated recently [6] is based on nanocrystallite quantum dots that can be produced with high reproducibility, of diameters $\sim 15 - 100\text{\AA}$ tunable during synthesis, with a narrow size distribution ($< 5\%$ rms). These dots can be forced to assemble into ordered three-dimensional closely packed colloidal crystals [6], with the structure of stacked two-dimensional triangular lattices. Due to higher flexibility and structural control, these systems are expected to be

good for studying effects inaccessible in the more traditional self-assembled quantum dot arrays fabricated using epitaxial growth techniques. In particular, the high charging energy of nanocrystallite dots, in the room temperature range, and the triangular lattice geometry of the dot arrays [6] are very interesting from the point of view of exploring novel kinds of charge ordering.

Motivated by recent attempts to bring charge carriers into these structures using gates, and to measure their transport properties [7], in this article we study charge transport in the classical Coulomb plasma on a triangular array of quantum dots. We assume that the dots can be charged by an external gate and that conducting electrons or holes can tunnel between neighboring dots.

For drawing a connection to the better studied spin systems, it is convenient to map this problem on the classical Ising antiferromagnet on a triangular lattice (Δ IAFM). Without loss of generality, we consider the case when the occupancy of the dots is either 1 or 0, and interpret these occupancies as the spin “up” and “down” states. In this language, the gate voltage is represented by an external magnetic field coupled to the spins. Also, more generally, any spatially varying electrostatic field is mapped on a spatially varying magnetic field in the spin problem. For example, the electrostatic field due to, e.g., charged defects, corresponds to the spin problem with a random field. The electron hopping (tunneling) between the dots corresponds to spin exchange transport. The long-range Coulomb interaction between charges gives rise to a long-range spin-spin coupling, which leads to somewhat different physical properties than the short-range exchange interaction conventional for the spin problems.

Another difference between the charge and spin problems is that, due to charge conservation, there is no analog of spin flips. This certainly has no effect on the equilibrium statistical mechanics, because the spin ensemble with fixed total spin is statistically equivalent to the grand canonical ensemble. However, this is known to be important in the dynamical problem [10]. The two corresponding types of dynamics are the spin conserving Kawasaki dynamics [11] and the spin non-conserving Glauber dynamics [12], respectively. In the simulation described below we use the Kawasaki dynamics, involving spin exchange processes on neighboring sites.

The mapping between the charge and spin problems is of interest because of the following. If the interaction between the dots were of a purely nearest neigh-

bor type, the problem could have been exactly mapped on the Δ IAFM problem, which is exactly solvable [8]. The Δ IAFM problem is known to have an infinitely degenerate ground state with an intrinsic “solid-on-solid” structure described by the so-called “height field” [9] (see below). The height field represents the correlations of occupancy of neighboring sites, and can be thought of in terms of an embedding of the structure into a three-dimensional space. The higher-dimensional representations of correlations in solids have also been found useful in a variety of frustrated spin problems [13]. The ordering of electrons in triangular arrays of quantum dots, because of Coulomb coupling giving rise to a repulsive nearest-neighbor interaction, must be similar to that of the Δ IAFM ground states. It represents, however, a new physical system in which the height field will be strongly coupled to electric currents, which can make electronic transport properties very interesting.

The Hamiltonian of the electrons on the quantum dots is given by $\mathcal{H}_{\text{charge}} + \mathcal{H}_{\text{tunnel}} + \mathcal{H}_{\text{spin}}$, where $\mathcal{H}_{\text{charge}}$ describes Coulomb interaction between charges $q_i = 0, 1$ on the dots and coupling to the background disorder potential $\phi(r)$ and to the gate potential V_g :

$$\mathcal{H}_{\text{charge}} = \frac{1}{2} \sum_{i,j} V(\mathbf{r}_{ij}) q_i q_j + \sum_{\mathbf{r}_i} (V_g + \phi(\mathbf{r}_i)) q_i \quad (1)$$

The position vectors \mathbf{r}_i run over a triangular lattice with the lattice constant a , and $\mathbf{r}_{ij} = \mathbf{r}_i - \mathbf{r}_j$. The interaction V accounts for screening by the gate:

$$V(\mathbf{r}_{ij} \neq 0) = \frac{e^2}{\epsilon |\mathbf{r}_{ij}|} - \frac{e^2}{\epsilon \sqrt{(\mathbf{r}_{ij})^2 + (2d)^2}}, \quad (2)$$

Here ϵ is the dielectric constant of the substrate¹, and d is the distance to the gate plate. The single dot charging energy $\frac{1}{2}V(0) = e^2/2C$ is assumed to be high enough to maintain no more than single occupancy.

Electron tunneling between neighboring dots is described by $\mathcal{H}_{\text{tunnel}}$. We assume that the tunneling is incoherent, i.e., is assisted by some energy relaxation mechanism, such as phonons. Below we consider stochastic dynamics in which charges can hop between neighboring dots with probabilities depending on the potentials of the dots and on temperature. Also, we consider only charge states and ignore all effects of electron spin described by $\mathcal{H}_{\text{spin}}$, such as exchange, spin ordering, etc.

To lay out the framework for discussing ordering in the charge problem, let us review here the main results

¹ In the case of spatially varying ϵ the interactions can be more complicated. For example, if the array of dots is placed over a semiconductor substrate, one has to replace $\epsilon \rightarrow (\epsilon + 1)/2$ in the expression (2).

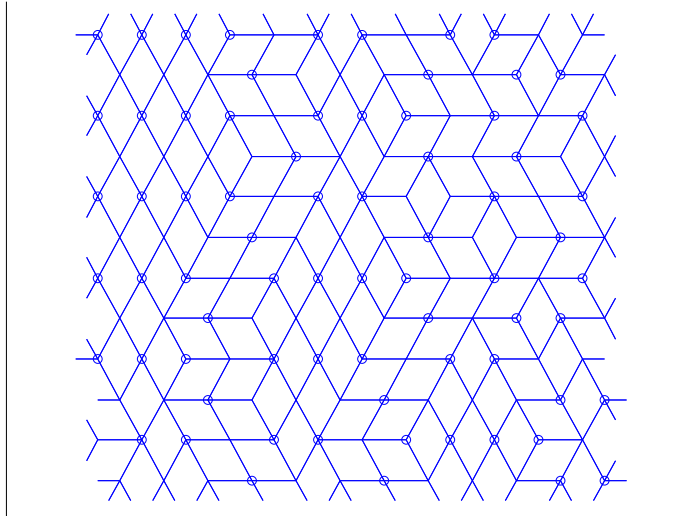


FIG. 1. Typical charge configuration obtained in a Monte Carlo simulation for the filling fraction $n = 1/2$. Pairing of the triangles is revealed by erasing all frustrated bonds connecting sites with equal occupancy.

for the Δ IAFM problem using the charge problem language (and assuming nearest neighbor interactions). The ground state of this system has a large degeneracy [8], which can be understood as follows. For each triangular plaquette at least one bond is frustrated, for any occupancy pattern. To minimize the energy of the nearest neighbor interactions, i.e., to reduce the number of frustrated bonds, it is favorable to arrange charges so that the triangles combine in pairs in such a way that each pair of triangles shares a common frustrated bond. The pairing of triangles can be described by partitioning the structure into rhombuses. Given a charge configuration, the corresponding rhombuses pattern can be visualized by erasing all frustrated bonds, as shown in Fig.1.

Conversely, given a configuration of rhombuses, one can reconstruct the arrangement of charges in a unique way, up to an overall sign change. The use of the representation involving rhombuses is that it leads to the notion of a height field. Any configuration of rhombuses can be thought of in terms of a projection of a faceted surface in a 3D cubic lattice along the (111) direction. This surface defines lifting of the 2D configuration in the 3D cubic lattice space, i.e., an integer-valued height field. The number of different surfaces that project onto the domain of area \mathcal{A} is of the order $e^{w\mathcal{A}}$, where w is a constant equal to the entropy of the ground state manifold per plaquette.

At a finite temperature, the charge ordering with respect to the height field, i.e., to the pairing of triangles, may have some defects (see Fig.2). An elementary defect is represented by an isolated unpaired triangle surrounded by rhombuses, i.e., by paired triangles. This

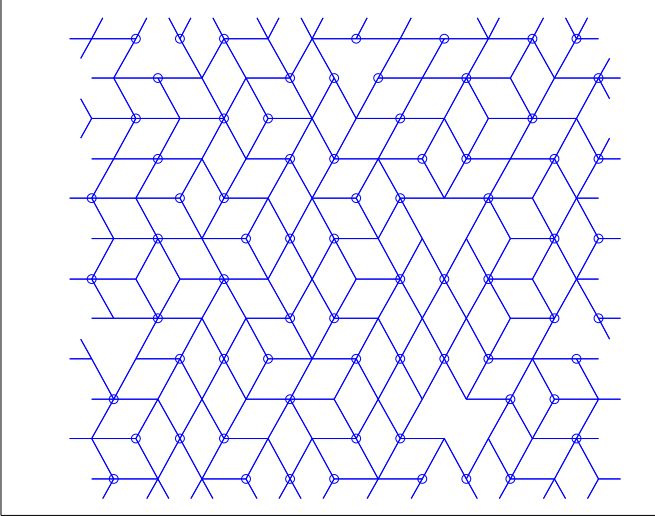


FIG. 2. Typical charge configuration for the filling fraction $n = 1/2$. In this case, the temperature is warmer than in Fig.1, and there are several defects (“screw dislocations”) present in the system.

defect has a topological character similar to a screw dislocation, because it leads to an ambiguity in the height field. This ambiguity is readily seen in Fig.2, where by continuing the height field around an unpaired triangle one finds a discrete change in it upon returning to the starting point.

There is no finite temperature phase transition in the Δ IAFM problem because of the topological defects present at a finite concentration at any temperature. However, since the fugacity of a defect scales as $e^{-V(a)/T}$, and the defect concentration scales with the fugacity, the system of defects is becoming very dilute as $T \rightarrow 0$. As a result, the $T = 0$ state is ordered, and belongs to the degenerate manifold of ground states without defects, i.e., is characterized by a globally defined height variable. Also, since the distance between defects diverges exponentially as $T \rightarrow 0$, there is a large correlation length for the $T = 0$ ordering even when T is finite. This situation is described in the literature on the Δ IAFM problem as a $T = 0$ critical point (see recent article [17] and references therein).

In this work, we study the charge system with the interaction (2) by a Monte Carlo (MC) simulation of electron hopping in equilibrium, as well as in the presence of an external electric field. We find that, although many aspects of the Δ IAFM physics are robust, the long-range character of the interaction (2) makes the charge problem different from the Δ IAFM problem in several ways.

The states undergoing the MC dynamics are all charge configurations with no more than single occupancy ($q_i = 0, 1$) on a square patch $N \times N$ of a triangular array ($N = 12$ in Figs.1,2,3). Periodic boundary conditions are imposed by defining the energy (1) using the $N \times N$

charge configuration extended periodically in the entire plane. Also, we allow charge hopping across the patch boundary, so that the charge disappearing on one side of the patch reappears on the opposite side, consistent with the periodicity condition.

The stochastic MC dynamics is defined by letting electrons hop on unoccupied neighboring sites with probabilities given by Boltzmann weights:

$$W_{i \rightarrow j} / W_{i \rightarrow i} = e^{(\Phi_i - \Phi_j) / kT}, \quad W_{i \rightarrow j} + W_{i \rightarrow i} = 1, \quad (3)$$

where

$$\Phi_i = \sum_{r_j \neq r_i} V(\mathbf{r}_{ij}) q_j + V_g + \phi(\mathbf{r}_i). \quad (4)$$

To reach an equilibrium at a low temperature, we take the usual precautions by running the MC dynamics first at some high temperature, and then gradually decreasing the temperature to the desired value.

All the work reported below was done on the system without disorder, $\phi(\mathbf{r}_i) = 0$. The distance to the gate which controls the range of the interaction (2) was chosen to be $d = 2$.

The properties of the system depend on the charge filling fraction, i.e., on the mean occupancy $n = \sum q_i / N^2$, which is conserved in the MC dynamics. (The Δ IAFM in the absence of external magnetic field corresponds to $n = 1/2$.) We find that at low temperature the equilibrium states with $1/3 \leq n \leq 2/3$ are very well described by pairing of the triangles, as illustrated in Figs.1,3. The defects with respect to this height field ordering have a very small concentration, if present at all. The short-range ordering in the charge problem turns out to be the same as in the Δ IAFM. Qualitatively, this similarity is explained by a relatively higher magnitude of the nearest neighbor coupling (2) compared to the coupling at larger distances.

Like in the Δ IAFM, we observe topological defects. They are present at warmer temperatures (see Fig.2) and quickly freeze out at colder temperatures (see Fig.1). The disappearance of the defects, because of their topological character, is possible only via annihilation of the opposite sign defects. An example of such a process can be seen in the lower right corner of Fig.2. The defects in the charge problem, besides carrying topological charge, can carry an electric charge. Two defects of opposite electric charge can be found at the top and on the left of Fig.2.

Expectedly, besides the robust features, such as the height field and the topological defects, there are certain non-robust aspects of the problem. The two most interesting issues that we discuss here are related with lifting of the degeneracy of the Δ IAFM ground state, and with the instability of the $T = 0$ critical point, both arising due to long-range coupling in the charge problem.

As we already have mentioned, the ground state manifold of the Δ IAFM is fully degenerate only for purely

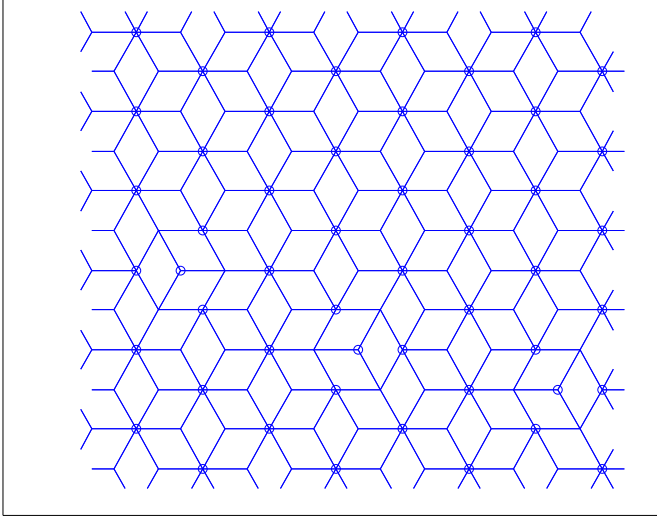


FIG. 3. Typical Monte Carlo charge configuration for $n = 1/3 + \epsilon$. There are three excess charges in the system ($\epsilon = 3/144$) hopping over the honeycomb network of unoccupied sites in the commensurate $\sqrt{3} \times \sqrt{3}$ state. The excess carriers, dilute at $\epsilon \ll 1$, are moving nearly independently on the background of the frozen $\sqrt{3} \times \sqrt{3}$ state.

nearest neighbor interactions. The degeneracy is lifted even by a weak non-nearest-neighbor interaction [14,15]. For instance, for our problem with the interaction (2) at $n = 1/2$, the favored ground states have the form of stripes, spaced by $\sqrt{3}$ in the lattice constraint units, which corresponds to electrons filling every other lattice row. Because there are three possible orientations of the stripes, the system cooled in the $n = 1/2$ state freezes in a state characterized by domains of the three types. One of such domains of stripes can be seen in the upper left part of Fig.1. Upon long annealing, the domains somewhat grow and occasionally coalesce. However, we were not able to determine whether the system always reaches a unique ground state, or remains in a polycrystalline state of intertwining domains.

This can be contrasted with the behavior at $n = 1/3$, where the ground state is a $\sqrt{3} \times \sqrt{3}$ triangular lattice, corresponding to electrons filling one of the three sublattices of the triangular lattice (see Fig.3). The rotational symmetry of this state is the same as that of the underlying lattice. Because there is a (triple) translational degeneracy of the ground state, but no orientational degeneracy, the system always forms a perfect triangular structure upon cooling, without domains. For the densities close to $1/3$, the ground state contains $|n - 1/3|$ charged defects, vacancies for $n < 1/3$ and interstitials for $n > 1/3$, formed on the background of the otherwise perfect $\sqrt{3} \times \sqrt{3}$ structure. At $n > 1/3$, the interstitials are moving over the honeycomb network of empty sites, as illustrated in Fig.3.

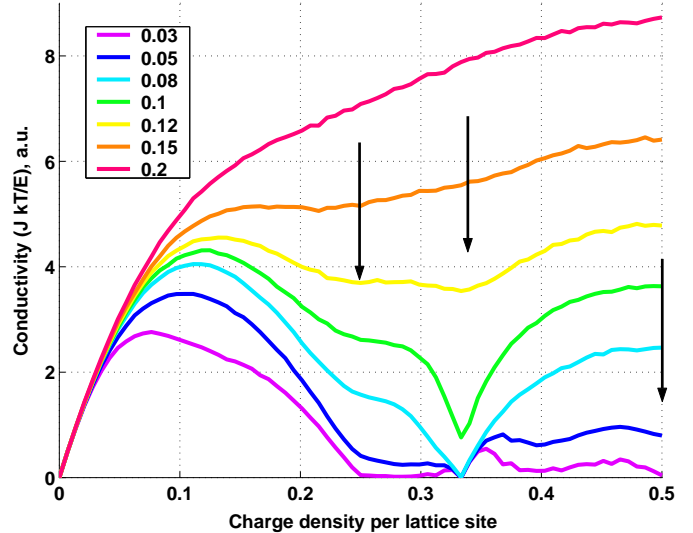


FIG. 4. Conductivity versus electron density for several temperatures, given in the units of $e^2/\epsilon a$. The density n varies from 0 (uncharged) to 1 (fully charged), however, because of the $n \leftrightarrow 1 - n$ symmetry, only the interval $0 \leq n \leq 1/2$ is displayed. Arrows mark the features corresponding to the phase transitions at $n = 1/3, 1/2, 1/4$.

Before discussing the issue of finite T versus $T = 0$ phase transitions, let us explain how we use the MC simulation to find electrical conductivity. It is straightforward to add an external electric field \mathbf{E} to the MC algorithm [16]. For that, one can simply modify the expressions (3) for the hopping probabilities by adding the field potential difference $\mathbf{E} \cdot (\mathbf{r}_{ij})$ between the two sites \mathbf{r}_i and \mathbf{r}_j . In doing this, one has to respect the periodic boundary condition, which amounts to taking the shortest distance between the sites \mathbf{r}_i and \mathbf{r}_j on the torus. Then the charges are statistically biased to hop along \mathbf{E} , which gives rise to a finite average current \mathbf{J} .

The current \mathbf{J} is Ohmic at small \mathbf{E} , and saturates at $|\mathbf{E}|a \geq \min(V(a)n^{1/2}, kT)$, where $a(n) = n^{-1/2}$ is the inter-electron spacing. Even though only the Ohmic regime $J \sim \mathbf{E}$ is of a practical interest, it is useful to maintain the field \mathbf{E} used in the MC simulation on the level of not less than few times below the nonlinearity offset field, to minimize the effect of statistical fluctuations on the time averaging of the current \mathbf{J} .

The dependence of the electric current on the density n is shown in Fig.4 for several temperatures. Because of the electron-hole symmetry of the system, the conductivity problem is invariant under the transformation $n \leftrightarrow 1 - n$, and thus only the interval $0 \leq n \leq 1/2$ can be considered. At high temperatures $kT \geq e^2/\epsilon a(n)$, the Coulomb interaction is not important, and one can evaluate the current by considering electrons freely hopping over lattice sites subject only to the single occupancy constraint. The current \mathbf{J} in this case goes as

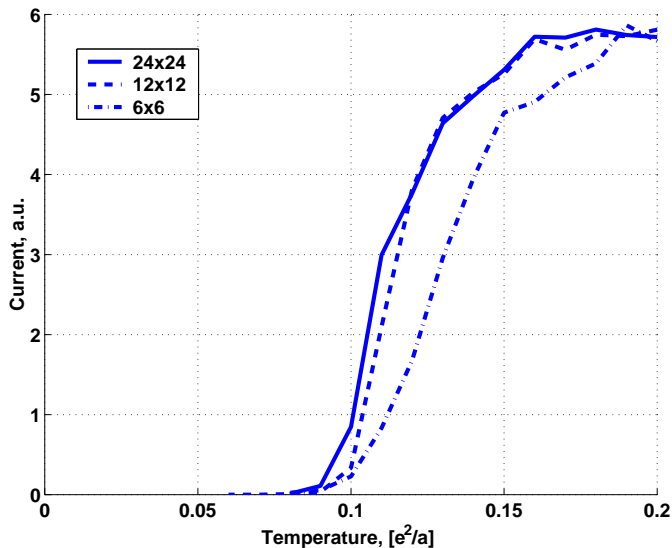


FIG. 5. Conductivity versus temperature for density $n = 1/3$. The three curves are obtained for three different system sizes.

$$\mathbf{J} = \frac{3}{4}n(1-n) \frac{\mathbf{E}}{kT}, \quad (5)$$

where the factor $n(1-n)$ in (5) gives the probability that a particular link connects two sites of different occupancy, so that hopping along this link can occur, whereas the factor (\mathbf{E}/kT) in (5) is the hopping probability bias due to the weak field $|\mathbf{E}| \ll kT$. The constant factor $3/4$ in (5) is given by the coordination number of the lattice (equal to 6) divided by 8.

The parabolic $n(1-n)$ dependence of the current (5) is clearly reproduced by the highest temperature curve in Fig.4. In Fig.4 the inverse temperature factor of the expression (5) is eliminated by rescaling the current by E/kT . The rescaled current $J(kT/E)$ in Fig.4 is practically temperature independent at small densities n , in agreement with the result (5). Regarding the $1/kT$ rescaling, note that in a real system the frequency of electron attempts to hop is a function of temperature, because hopping is assisted by energy relaxation processes, such as phonons. In this case, our MC result for the current \mathbf{J} has to be multiplied by some function $A(T)$, which will be of a power law form T^α for the phonon absorption rate in the case of a phonon-assisted hopping.

At the temperatures of the order and smaller than $e^2/\epsilon a(n)$, the current becomes suppressed due to charge correlations reducing the frequency of hopping. The onset of this suppression takes place at temperatures of order of the interaction between neighboring electrons, $kT \simeq 0.2V(a)n^{1/2}$. Note that the onset temperature is lower for smaller density, in agreement with the plots in Fig.4.

The electrical conductivity is a sensitive probe of freezing transitions, at which the system of interacting charges

locks collectively into a particular ordered or disordered state, and the conductivity vanishes. Whether the freezing occurs as a finite T or a $T = 0$ phase transition is related to the degree of degeneracy of the ground state. The situation appears to be very different at different densities n . For simple rational $n = 1/3, 1/2, 2/3$, and alike, characterized by the ground state unique up to discrete symmetries, there is a well defined freezing temperature. This is illustrated in Fig.5, where electrical conductivity of the $n = 1/3$ state is plotted versus temperature. The abrupt drop of the conductivity at $kT \approx 0.09e^2/\epsilon a$, where a is the lattice constant, indicates a sharp freezing transition. To make sure that this is not a finite size effect, we show the conductivity curves for systems of three different sizes, 6×6 , 12×12 , and 24×24 .

On the other hand, away from the specific densities with simple ground states, the freezing appears to be very gradual, and in the temperature range we explored in Fig.4 there has been no evidence of a sharp transition. It may be that the ordering actually takes place at much smaller temperatures than the characteristic interaction, the situation not uncommon in frustrated systems. Also, it may be that at incommensurate densities the state remains disordered down to $T = 0$. From our observations, the latter seems to be a more likely scenario. We expect that upon cooling the charges freeze into a quasirandom state determined by the cooling history. In that case, this system represents an electronic glass that exists in the absence of external disorder.

The nature of the ground state in this case is unclear. To list several options, it may be that the system forms a polycrystal consisting of intertwining domains, like it does at $n = 1/2$, or that the state represents a distorted incommensurate charge density wave, or that it is a genuine glass. Studying this would require enhancing the MC algorithm to make it capable of treating the slow dynamics of annealing at low temperatures.

In conclusion, correlations of charges in the triangular arrays are described by an intrinsic order parameter, the height field, similar to the Δ IAFM problem. The charge-spin mapping shows that various interesting phenomena arising in frustrated spin systems can be studied in charge systems, for which more powerful experimental techniques are available. The type of order in the ground state depends on the charge filling density. Electron hopping conductivity is sensitive to charge ordering and can be used as a probe of the nature of the ordered state. Conductivity couples to the height field, and thus one can expect novel effects in electronic transport properties which have no analog in spin systems with the same geometry.

ACKNOWLEDGMENTS

We are very grateful to Marc Kastner, Mounqi Bawendi, and Nicole Morgan for drawing our attention to this problem, as well as for many useful discussions and for sharing with us their unpublished experimental results. This work is supported by the NSF Award 67436000IRG.

-
- [1] J.E.Mooij, G.Schön, in *Single Charge Tunneling*, eds H.Grabert and M.H.Devoret, (Plenum, New York, 1992), Chapter 8 and references therein; Proceedings of the NATO Advanced research Workshop on Coherence in Superconducting Networks, Delft, eds. J.E.Mooij, G.Schön, *Physica* **142**, 1-302 (1988); H.S.J.van der Zant, et al., *Phys.Rev.B***54**, 10081 (1996); A.van Oudenaarden, *Phys.Rev.Lett.***76**, 4947 (1996)
- [2] D.Heitmann, J.P.Kotthaus, *Phys.Today* **46** (1), 56 (1993); H.Z.Xu, W.H.Jiang, B.Xu, et al., *J.Cryst.Growth* **206** (4), 279-286 (1999), and *ibid.* *J.Cryst.Growth* **205** (4), 481-488 (1999)
- [3] S.Teitel, C.Jayaprakash, *Phys.Rev.Lett.* **51**, 1999 (1983); T.C.Halsey, *J.Phys. C* **18**, 2437 (1985); S.E.Korshunov, G.V.Uimin, *J.Stat.Phys.* **43**, 1 (1986); S.E.Korshunov, *ibid.* **43**, 17 (1986); E.Granato, J.M.Kosterlitz, J.Lee, and M.P.Nightingale, *Phys.Rev.Lett.* **66**, 1090 (1991); J.-R.Lee, S.Teitel, *Phys.Rev.Lett.* **66**, 2100 (1991);
- [4] A.I.Yakimov, et al, *J.Phys. C* **11** (48) 9715-9722 (1999); *Phys.Low-Dimens.Str.* 3-4: 99-109 (1999); E.Ribeiro, E.Muller, T.Heinzel, H.Auderset, K.Ensslin, G.Medeiros-Ribeiro, P.M.Petroff, *Phys.Rev. B***58**, 1506 (1998)
- [5] A.Groshev, G.Schön, *Physica B* **189** (1-4), 157-164 (1993); T.Takagahara, *Optoelect.Dev.Tech.* **8**, 545 (1993); *Surf.Sci.***267**, 310 (1992); G.Medeiros-Ribeiro, F.G.Pikus, P.M.Petroff, A.L.Efros, *Phys.Rev. B***55**, 1568 (1997); O.Heller, P.Lelong, G.Bastard, *Physica B* **251**, 271-275 (1998)
- [6] C.B.Murray, C.R.Kagan, M.G.Bawendi, *Science* **270**(5240) p. 1335 (1995); C.B.Murray, D.J.Norris, and M.G.Bawendi, *J.Am.Chem.Soc.***115**, 8706 (1993)
- [7] M.A.Kastner, N.Y.Morgan (private communication)
- [8] G.H.Wannier, *Phys.Rev.* **79**, 357 (1950); J.Stephenson, *J.Math.Phys.* **5**, 1009 (1964); *J.Math.Phys.* **11**, 413 (1970)
- [9] H.W.J.Blöte and H.J.Hilhorst, *J.Phys. A***15**, L631 (1982); B.Nienhuis, H.J.Hilhorst, and H.W.J.Blöte, *J.Phys. A***17**, 3559 (1984)
- [10] P.C.Hohenberg, B.I.Halperin, *Rev.Mod.Phys.***49**, 435 (1977)
- [11] K.Kawasaki, *Phys.Rev.***148**, 375 (1966); K.Kawasaki, in *Phase Transitions and Critical Phenomena*, C.Domb and M.S.Green, eds, Vol.2 (Academic Press, London, 1972)
- [12] R.J.Glauber, *J.Math.Phys.***4**, 294 (1963)
- [13] W.Zheng and S.Sachdev, *Phys.Rev. B***40**, 2704 (1989); L.S.Levitov, *Phys.Rev.Lett.* **64**, 92 (1990); S.Sachdev and N.Read, *Phys.Rev.Lett.* **77**, 4800 (1996)
- [14] S.L.A.de Queiroz and E.Domany, *Phys.Rev. E***52**, 4768 (1995)
- [15] C.Zeng and C.L.Henley, *Phys.Rev. B***55**, 14935 (1997)
- [16] J.-R.Lee, S.Teitel, *Phys.Rev. B***50**, 3149 (1994);
- [17] Hui Yin, Nicholas Gross, Bulbul Chakraborty, Effective Field Theory of the Zero-Temperature Triangular-Lattice Antiferromagnet: A Monte Carlo Study, condmat/9911129 preprint